Seasonal snowpack microbial ecology and biogeochemistry on a High Arctic ice cap reveals negligible autotrophic activity during spring and summer melt

Archana Dayal[1], Andrew Hodson[2], Marie Sabacka[3], and Alan L Smalley[4]

[1]Aberystwyth University
[2]University Centre in Svalbard
[3]University of South Bohemia in České Budějovice
[4]The University of Sheffield

September 13, 2022

Abstract

Snowpack ecosystem studies are primarily derived from research on snow-on-soil ecosystems. Greater research attention needs to be directed to the study of glacial snow covers as most snow cover lies on glaciers and ice sheets. With rising temperatures, snowpacks are getting wetter, which can potentially give rise to biologically productive snowpacks. The present study set out to determine the linkage between the thermal evolution of a snowpack and the seasonal microbial ecology of snow. We present the first comprehensive study of the seasonal microbial activity and biogeochemistry within a melting glacial snowpack on a High Arctic ice cap, Foxfonna, in Svalbard. Nutrients from winter atmospheric bulk deposition were supplemented by dust fertilisation and weathering processes. NH4+ and PO43- resources in the snow therefore reached their highest values during late June and early July, at 22 and 13.9 mg m-2, respectively. However, primary production did not respond to this nutrient resource due to an absence of autotrophs in the snowpack. The average autotrophic abundance on the ice cap throughout the melt season was 0.5 {plus minus} 2.7 cells mL-1. Instead, the microbial cell abundance was dominated by bacterial cells that increased from an average of (39 {plus minus} 19 cells mL-1) in June to (363 {plus minus} 595 cells mL-1) in early July. Thus, the total seasonal biological production on Foxfonna was estimated at 153 mg C m-2, and the glacial snowpack microbial ecosystem was identified as net-heterotrophic. This work presents a seasonal 'album' documenting the bacterial ecology of glacial snowpacks.

Seasonal snowpack microbial ecology and biogeochemistry on a High Arctic ice cap reveals negligible autotrophic activity during spring and summer melt

A. Dayal[1], A.J. Hodson[2,3], M. Šabacká[4] and A. L. Smalley[5]

[1]Institute of Biological, Environmental & Rural Sciences, Aberystwyth University, Aberystwyth, UK. [2]Arctic Geology Department, University Centre in Svalbard, Longyearbyen, Norway. [3]Department of Environmental Sciences, Western Norway University of Applied Sciences, Sogndal, Norway. [4]Centre for Polar Ecology, University of South Bohemia, Czech Republic. [5]Department of Geography, University of Sheffield, UK.

Corresponding author: Archana Dayal (ard33@aber.ac.uk)

Key Points:

- Nutrients delivered by snow from marine and continental sources were supplemented by the dissolution of dust deposited from local sources
- Autotrophic communities were conspicuous by their absence within a High Arctic glacial snowpack during summer
- Secondary bacterial production therefore dominated the entire summer
- A superimposed ice layer of refrozen snowmelt acted as a temporary dilute store for nutrients and cells

Abstract

Snowpack ecosystem studies are primarily derived from research on snow-on-soil ecosystems. Greater research attention needs to be directed to the study of glacial snow covers as most snow cover lies on glaciers and ice sheets. With rising temperatures, snowpacks are getting wetter, which can potentially give rise to biologically productive snowpacks. The present study set out to determine the linkage between the thermal evolution of a snowpack and the seasonal microbial ecology of snow. We present the first comprehensive study of the seasonal microbial activity and biogeochemistry within a melting glacial snowpack on a High Arctic ice cap, Foxfonna, in Svalbard. Nutrients from winter atmospheric bulk deposition were supplemented by dust fertilisation and weathering processes. NH_4^+ and PO_4^{3-} resources in the snow therefore reached their highest values during late June and early July, at 22 and 13.9 mg m^{-2}, respectively. However, primary production did not respond to this nutrient resource due to an absence of autotrophs in the snowpack. The average autotrophic abundance on the ice cap throughout the melt season was 0.5 ± 2.7 cells mL^{-1}. Instead, the microbial cell abundance was dominated by bacterial cells that increased from an average of (39 ± 19 cells mL^{-1}) in June to (363 ± 595 cells mL^{-1}) in early July. Thus, the total seasonal biological production on Foxfonna was estimated at 153 mg C m^{-2}, and the glacial snowpack microbial ecosystem was identified as net-heterotrophic. This work presents a seasonal 'album' documenting the bacterial ecology of glacial snowpacks.

Plain language summary

Most research attention has been given to snow covers lying on top of soil ecosystems, and therefore we do not know enough about the ecology of glacial snowpack ecosystems. This is a major knowledge gap, given that most of the world's snow cover lies over glaciers, ice caps and ice sheets. This study shows that during the melt season on a High Arctic ice cap, Foxfonna in Svalbard, nutrients are most available during the peak of summer (June to early July transition period), but a shortage of photosynthesising microbes can mean that they largely remain in situ until transported downstream by meltwater runoff. Processes with the capacity to generate high concentrations of essential nutrients such as N and P in snow and meltwater could therefore be described, because the primary producers did not sequester them. In contrast, an increase in bacterial cell numbers was observed during the same period. The glacial snowpack ecosystem was therefore net-heterotrophic due to the absence of autotrophs and proliferation of bacterial cells. Since the nutrient demand of the bacterial biomass is low, the ecosystem releases carbon, nitrogen, and phosphorus, rather than fixes it.

1 Introduction

1.1 The status of glacier snowpack ecosystem research

Seasonal snowpacks cover nearly a third of the Earth's land surface at the start of summer with a mean winter maximum extent of 47 x 10^6 km^2 (Hinkler *et al.*, 2008). Snow covers play an integral role in the climate system via radiative feedbacks, ground insulation (Hinkler *et al.*, 2008) and biogeochemical cycles (Wadham *et al.*, 2013). Although snowpacks have received significant research attention, most has been in the context of snow covers lying on top of soil or other aquatic ecosystems (Jones *et al.*, 1999; Kuhn, 2001; Larose *et al.*, 2010; Larose, Dommergue and Vogel, 2013).

What is known about glacial snowpack ecosystems is largely derived from molecular, functional, and physiological studies (e.g., Lutz *et al.*, 2016; Malard *et al.* 2019; Hoham and Remias, 2020). These studies have given a great deal of attention to snow algae and glacier algae, not least due to their linkage with pigment-mediated albedo reduction and melt enhancement (Williamson *et al.*, 2019; Cook *et al.*, 2020; Gray *et al.*, 2020; Mauro *et al.*, 2020). Recently, there has been a shift from the aforementioned studies to the study of interactions between algae, fungi and bacteria (Krug *et al.*, 2020; Fiołka *et al.*, 2021). Although important, such approaches have offered little understanding of fundamental ecosystem characteristics, such as links to biogeochemical processes and the changing physical conditions of a snowpack during melt.

We are yet to understand the (re)distribution of nutrients and microbes within the different layers of a melting snowpack and how this supports the concept of the snowpack as an ecosystem, especially in the context of changing climate. From this perspective, it is expected that surface meltwater will play a critical role in the redistribution of microbes and nutrients on the surface of glaciers, including their delivery to the deeper (darker) layers of the snowpack or the glacier bed, where photosynthesis cannot occur, and heterotrophic production is likely to be dominant (e.g., (Skidmore *et al.*, 2000; Mikucki and Priscu, 2007). Additionally, one can expect the ecology of snow to be driven by the production of meltwater and the changes in the snowpack's physical condition during melt because this greatly affects the propagation of light through the snow and the transfer of nutrients by percolating liquid water (e.g. Tranter and Jones, 2001; Hodson *et al.*, 2017). We, therefore, hypothesise that with the evolution in a snowpack's physical condition during summer melt, greater heterogeneity will be expected in microbial abundance and nutrients within the different layers of a melting snowpack (see also Nowak *et al.*, 2018).

In addition to increased melting, the warming of the cryosphere is also changing the composition of snowpacks. For example, a surface energy/mass balance model of an Arctic glacier (Wright *et al.*, 2007) predicted that due to rising temperatures, superimposed ice (formed following the refreezing of meltwater) will account for greater than 50% of the total accumulation by 2050. Furthermore, this superimposed ice has been shown to be a transient reservoir of nutrients/organic carbon in an earlier study on the Foxfonna ice cap (Kozioł *et al.*, 2014, 2019). In addition, Hell *et al.*, 2013 demonstrated that the microbial communities within the melting snowpack were structured according to habitat type, i.e., most taxa showed different distributions based on the habitat (surface snow, snow, slush and near-surface ice). This niche specificity was also demonstrated in a maritime Antarctic (Livingston Island) glacial snowpack where Hodson *et al.*, (2017) provided evidence for differences detectable not only in the microbial community

composition, but also the biomass and nutrients of coastal and inland (glacial) snowpacks, thereby highlighting changes over short distances (<1 km). A new study, carried out upon another maritime Antarctic glacier (Signy Island), also revealed such differences between two coastal sites, as well as within the vertical profile of a glacial snowpack with a substantial superimposed ice layer (Hodson *et al.*, 2021). In this context, snowpack stratification and its effects on resident microbes and nutrients could be significant. Therefore, this study will examine the ability of superimposed ice to form a unique habitat or niche for microbial life.

To date, carbon balance studies in snowpacks lag behind studies in other glacial habitats, especially cryoconite holes, supraglacial streams and lakes (e.g., Cook et al., 2012; Dubnick et al., 2017). This is in spite of snowpacks being a recognised organic carbon reservoir (Priscu et al., 2008) with the ability to influence air-snow exchange processes (Amoroso *et al.*, 2010), downstream ecosystems (Hood *et al.*, 2015) and the carbon cycle (Wadham *et al.*, 2019). Even fewer attempts have been made to integrate carbon into an ecosystem model that can help us understand the sources, sinks and transformations, and these have focused upon either surface glacial ice or cryoconite (e.g., Hodson *et al.*, 2010; Cook *et al.*, 2012; Stibal, Bradley and Box, 2017). In this study, biomass carbon will therefore be estimated, and its application to the quantification of autotrophic and heterotrophic microbial production duly considered.

We therefore present the first comprehensive study of the microbial activity and biogeochemistry of a melting snowpack on a High Arctic ice cap, Foxfonna. In so doing, we characterise seasonal changes in microbial abundance, nutrient and chlorophyll concentrations within snow, superimposed ice and glacial ice. Once the seasonal ecology of a melting snowpack on Foxfonna has been established, autotrophic and bacterial production rates are investigated by estimating cellular biomass change.

2 Materials and Methods

2.1 Study site

Foxfonna (78º07´-78º09´N; 16º06´-16º11´E) is a small (4 km^2) mountain ice cap in Central Spitsbergen, Svalbard (Figure 1), 2.31 km in diameter with elevations mainly between 550 and 808 m.a.s.l. (Kozioł 2014). Ground-penetrating radar surveys on Foxfonna show glacial ice that is less than 80 m thick (Murray, T., Unpublished Data in Rutter *et al.*, 2011). These surveys suggested that the ice cap is cold-based, as was established following the measurement of negative temperatures in boreholes beneath its North Outlet (Liestøl, 1993).

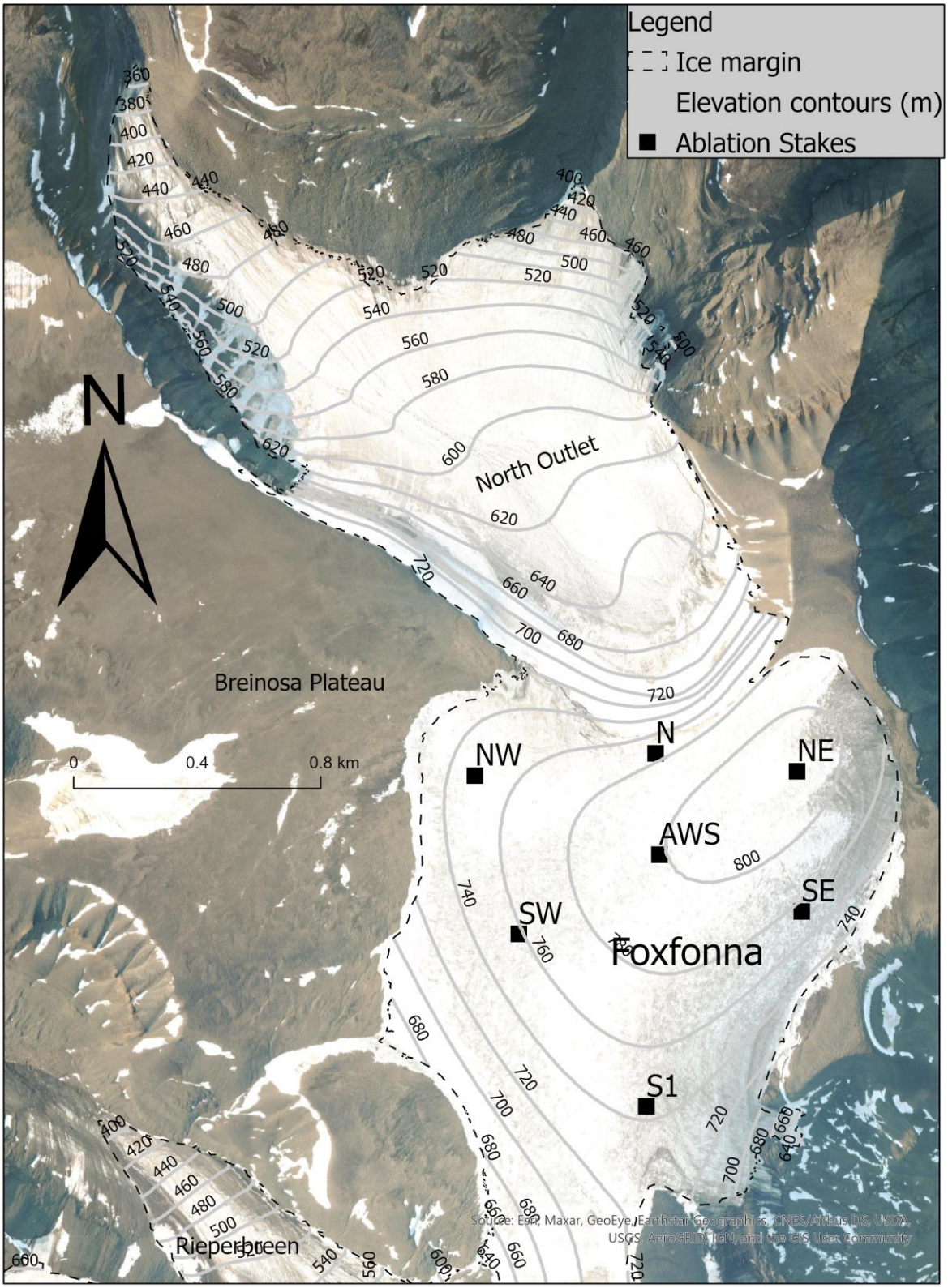

Figure 1. Foxfonna ice cap on Svalbard with ice margins and sampling sites marked.

2.2 Snow pit sampling

Figure 2 presents the key changes in snow depth and thermal conditions observed during the melt season at Foxfonna, from April (pre-melt) to late July. In April, the snowpack was dry and cold with a depth of ~1.5 m (at most sites). In addition, a layer of metamorphosed snow developed between the glacial ice and the overlying snowpack due to vapour and temperature gradients during the cold period.

A key transition period (hereafter "T1") involved the development of a wet and larger, coarse-grained snow surface as energy became available in response to the onset of summer, during June. Although some minor melting occurred at the surface, snow temperatures remained below freezing beneath it. The second important transition period, "T2", from June to early July, was marked by increasing temperatures, enhanced snowmelt and meltwater percolation to the bottom of the snow, where refreezing occurred. The growth and development of superimposed ice at the snow-glacier interface occurred during this period (when ice lenses also formed within cold snow patches above it). Collectively, these processes removed the "cold content" of the snowpack and brought the entire column up to the melting point. Thereafter, the isothermal melting snowpack slowly melted, forming slush or basal meltwater and runoff, before exposing the underlying layer of superimposed ice in July (transition period "T3"). Loss of this exposed superimposed ice as runoff occurred by late July. Typically, a slushy mix of larger coarse-grained snow crystals, residual superimposed ice and glacial ice was observed by this time, and glacier surface debris (cryoconite) became obvious.

Field campaigns were therefore undertaken in 2016 for the purpose of a pre-melt survey (April) and to coincide with transition periods: T1 in June, T2 in early July and T3 in late July (see Figure 2). Based on the directional aspect of Foxfonna, seven stakes (NW, SW, S1, AWS, SE, NE and N) were chosen for snow pit sampling (Figure 1). At each of the seven stakes, the following samples were collected into sterile Whirl-pak (*Nasco*) bags: surface snow (0 – 20 cm depth), mid snow (from 20 cm depth to the base of the snowpack), superimposed basal ice and the underlying glacier ice. These samples are hereafter referred to respectively as "TOP, MID, SUP ICE and GL ICE". Samples in April and June were collected using a pre-cleaned 8.5 cm diameter Federal Snow Sampling Tube (Rickly Hydrological Co.). In July, the presence of slush and thick superimposed ice required the use of a KOVACS Mark V ice corer (14 cm inner diameter) along with snow pit sampling. A consistent core length of 25 cm GL ICE was extracted at each stake (Figure 1) during the early and late July surveys only.

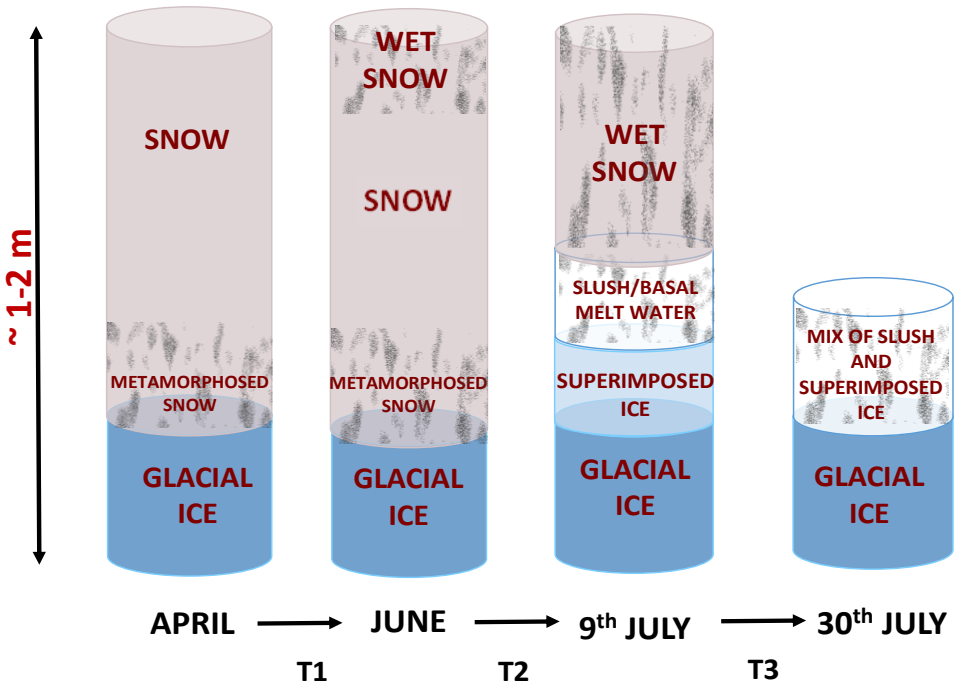

Figure 2. A schematic diagram showing the change in Foxfonna snowpack profile observed as melt season progressed from April (pre-melt to late July, 2016). Transition periods marked as T1, T2, T3.

2.3 Biogeochemical parameters

Samples were stored frozen in sterile 1L Whirl-paks (*Nasco*) at -20ºC until their pre-processing at the University Centre in Svalbard (UNIS). To minimise biogeochemical changes, all the samples were melted in the dark at ambient room temperature. Powder-free nitrile gloves were used to handle all samples.

After thaw, samples were agitated and a 10 mL aliquot was immediately removed for a UV-based chlorophyll *a* fluorescence measurement. This was done using a Chelsea Unilux fluorimeter with a notional detection limit of 0.01 µg L^{-1} and the average of 3 fluorescence readings were taken. pH measurements were conducted using a standard, portable meter and electrodes (Hanna Instruments, UK) calibrated using new pH 4 and 7 buffers. For microscopy analysis, 13 mL of subsample was removed using a sterile syringe, fixed with 1 mL of 0.2 µm-filtered 1% formalin and stored in sterile 15 mL Corning centrifuge tubes. The samples for microscopy were stored in the dark at 4ºC until further analysis at the University of Sheffield, UK.

Analysis of other biogeochemical parameters such as nutrients and cell pigments required filtration. For nutrient analysis, 25- mL aliquots were filtered through 0.45 µm Whatman glass fibre filter paper (47 mm) using a glass filtration apparatus (acid-washed with 10% HCl). Filtered samples were stored in sterile 50 mL conical centrifuge tubes (VWR). Concentrations of cations Na^+, K^+, Mg^{2+}, Ca^{2+} and anions Cl^-, F^- and SO_4^{2-} were determined using the Dionex ICS90 ion

chromatography, calibrated in the range 0.01-1 mg L^{-1} for cations and in the range 0.25-1 mg L^{-1} for anions. The precision errors for these ions ranged from 0.9% to 1.6%, while the detection limit was ≤ 0.05 mg L^{-1} (calculated as three times the standard deviation of ten blanks). Quantification of NH_4^+, PO_4^{3-}, NO_3^- and Si in the samples were conducted using a Skalar San++ Continuous Flow Analyser, calibrated in the range 0-3 mg L^{-1}. The limit of detection for these ions was ≤ 0.05 mg L^{-1} (calculated as three times the standard deviation of ten blanks), while the limit of quantification was ≤ 0.2 mg L^{-1}. These analyses employed standard colorimetric methods (based on The European Standard EN ISO, 1996, 2002, 2004 and 2005). Data for other ions analysed such as Na^+, K^+, Mg^{2+}, Ca^{2+}, F^-, SO_4^{2-}, Si and DOC are not shown (see Supplementary Tables S1 – S4) and are only discussed in the context of factor analysis of the entire data set (Section 3.2).

2.4 Pigment concentration

Melted samples (up to 420 mL) were filtered onto 0.45 µm Whatman glass fibre filter paper (47 mm). Filters were individually wrapped in aluminium foil and returned frozen to the UK for analysis. Further, frozen filter papers were transported insulated with reusable refrigerant polar gel packs (ThermoSafe®) in a polystyrene box to the University of Bristol and immediately stored at -80°C. Filters were then freeze-dried (for 24 hours), and High-Performance Liquid Chromatography (HPLC) analysis of the samples was undertaken following procedures described in Williamson et al. (2018, 2020).

2.5 Epifluorescence microscopy for cell counts

The glass filtration set-up was rinsed and cleaned with 70% ethanol prior to analysis and in-between samples to avoid contamination. Ten mL of sample was filtered through a 0.2 µm Poretics Polycarbonate Track Etched Black (25 mm, *Life Sciences*) filter paper, processed, followed by the addition of a combination of SYBR Green II (*Molecular Probes*) and Propidium Iodide (PI, *Invitrogen)* stains. The stain combination comprised of 10 µL of SYBR Green II (1x working solution) and 5 µL of 1.5 mM PI prepared in 1 mL of Dimethyl Sulfoxide (DMSO) solution. The dual stained sample was allowed to incubate for 15 minutes in the dark and was then filtered. This dual-stained approach was developed from flow cytometric viability studies on freshwater and marine bacteria (Lebaron, Parthuisot and Catala, 1988; Barbesti *et al.*, 2000; Grégori *et al.*, 2001) as well as live/dead cell counts of bacteria in drinking water (Sysmex, Partec). The filter paper was then placed onto a glass side, a drop of SlowFade® Diamond Antifade Mountant added to it, excess fluid removed and then covered with a coverslip, ready for imaging.

For bacterial cell counts, a Widefield Nikon Live-Cell System was used at 100x magnification, and microscopic fields were captured to count a minimum of 300 cells (Cook et al., 2020), which was not always possible (e.g. for clean snow samples). The stained samples were excited at 470 nm and detected via filter cubes. Autotrophic cell counts were undertaken at 20x, 40x and 63x and viewed under UV (for chlorophyll *a* fluorescence) and bright-field.

After imaging, images were converted to 8-bit greyscale on the software ImageJ. Cells were counted using the *Analyze Particles* function with a size range of 0.2 to 2 μm^2 and a circularity of 0 to 1. This was done to exclude the counting of mineral debris and remove noise. Filamentous bacteria or snow algae were measured manually on the software, as they were larger (10 – 20 µm). The cell counts (cells mL^{-1}) were calculated as a product of the counts per image and the microscope's field of view (FOV), divided by the volume of the sample filtered.

3 Results

3.1 Seasonal change in snow cover, nutrients, cells and chlorophyll on Foxfonna

The glacier mass balance conditions that were experienced during the study included the joint highest (i.e., 54 cm w.e.) winter snow accumulation since records began in 2007. The summer ablation was the fourth highest for the same interval (average-119 cm w.e.), causing a near-complete disappearance of the snowpack during the summer that is rather typical of this site. Figure 3A shows the evolution of the average snow water equivalent (SWE) through the melt season. Average values for the seven stakes ranged from 53 - 56 cm water equivalent (w.e.) from April until early July, and then dropped to 8 cm w.e. by the end of July (including any residual superimposed ice): most of which was near Stake N. Growth of superimposed ice commenced during T2 (June to early July) and formed an average water equivalent of 11 ± 5.4 cm w.e. (not shown). Depletion of combined snow and superimposed ice to 1 ± 2.5 cm w.e. occurred during transition period T3 (early to late July), according to the late July survey. In late July, the high standard deviation was due to superimposed ice being left at only one stake (AWS).

Nutrient loading at each stake was calculated from the product of the SWE (cm w.e.) of separate TOP, MID and SUP ICE samples and their corresponding nutrient concentration (mg L^{-1}), which were then summed to produce the total mass (or "loading") at each stake location in mg m^{-2}. Averages of these nutrient loading values at the stakes were then estimated for each survey to reveal seasonal changes across the entire ice cap. Comparison between SWE and Cl^- loadings (Figure 3 A and B) show leaching of Cl^- from the snowpack between June and early July (i.e. transition period T2), because the Cl^- loading decreased more rapidly than SWE. Average Cl^- loadings for the entire ice cap stayed below 1000 mg m^{-2} with the lowest value observed at the end of July: 53 ± 85 mg m^{-2}. By comparison, loadings of NH_4^+ and PO_4^{3-} were as much as two orders of magnitude lower, as is expected in such an oligotrophic environment. NH_4^+ ranged from 1 - 22 mg m^{-2} and PO_4^{3-} ranged even lower, at 0.4 - 13.9 mg m^{-2} through the melt season. Interestingly, during T2 (June – early July), NH_4^+ and PO_4^{3-} loadings increased whilst Cl^- and NO_3^- decreased. In fact, NH_4^+ and PO_4^{3-} loadings reached their highest values sometime after the onset of significant melting during early July at 22 and 13.9 mg $m^{-2,}$ respectively. Surprisingly, NO_3^- did not show its highest loading at the same time as NH_4^+. Instead, NO_3^- was leached rather like Cl^- and ranged from 0.5 - 15.4 mg m^{-2}.

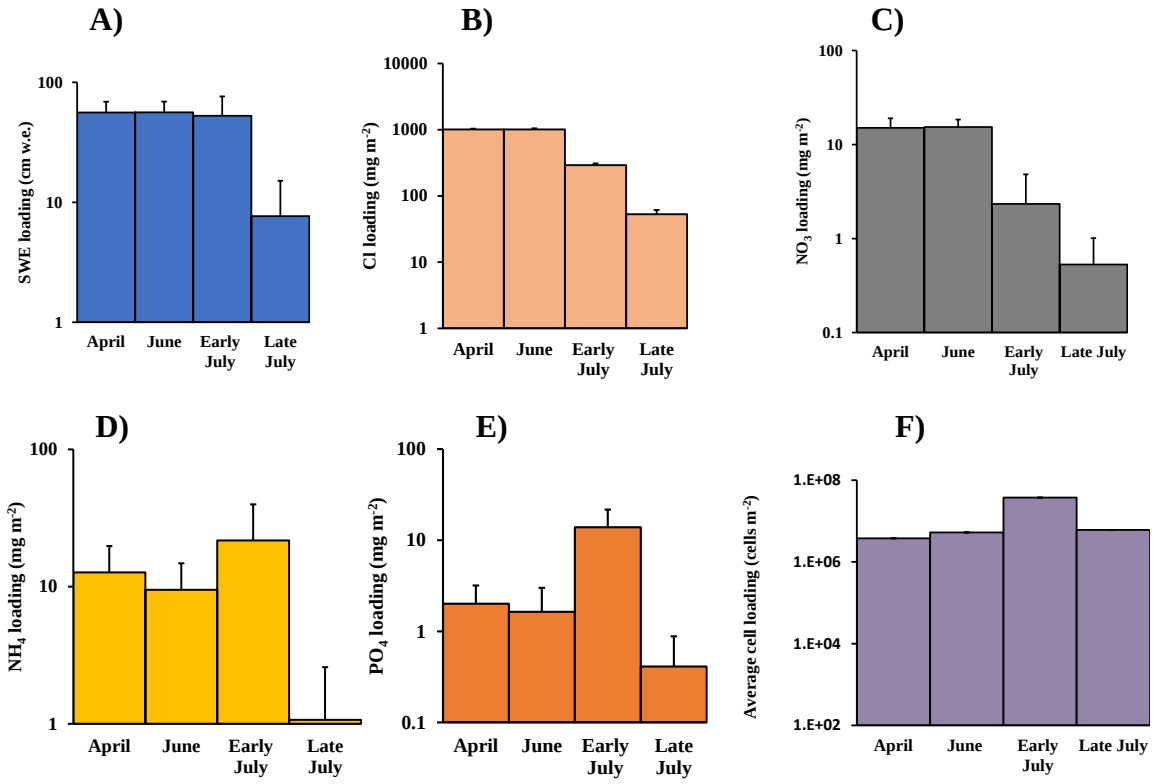

Figure 3. Seasonal change in Snow Water Equivalent (SWE), average loadings (mg m^{-2}) for Cl^-, NO_3^-, NH_4^+, PO_4^{3-} and cell loading on Foxfonna ice cap. Error bars are standard deviations (n=7)

Bacterial cell loading (cells m^{-2}) at each stake was calculated in an identical manner to the nutrient loading estimates (Figure 3F). Seasonal variations in the average cell loading across Foxfonna revealed minimal change during transition period T1, a significant increase (p-value = 0.05 where $\alpha = 0.05$) from 5.3 x 10^6 (± 2.7 x 10^5) to 3.8 x 10^7 (± 4.3 x 10^6) cells m^{-2} occurred during transition period T2 (June to early July). A decrease to 6.1 x 10^6 (± 1.6 x 10^6) cells m^{-2} followed during T3 (early to late July), although this was insignificant at the 95% confidence level (p-value = 0.3 where $\alpha = 0.05$), due to strong spatial variability in cell concentrations.

Chlorophyll *a* was the dominant pigment within snow, superimposed ice and glacial ice (Supplementary Figure S2). The Unilux derived chlorophyll *a* concentration within snow, superimposed ice and glacier ice ranged between 1.7 and 13 µg L^{-1} (Supplementary Figure S3). There was no significant change within the TOP and MID snows during transition periods T1 and T2, i.e., between April and June, where it lay in the range 1.7 – 2.7 µg L^{-1} and from June to early July, 1.7 – 1.9 µg L^{-1}. GL ICE displayed the highest chlorophyll *a* concentration at 13 µg L^{-1} and 10.7 µg L^{-1} in early and late July, respectively. However, when the snow samples were examined under the microscope, no autotrophic cells were detected in most samples. A slight increase in the cell numbers, e.g., to 25 cells mL^{-1}, yielded chlorophyll *a* concentration of 3 µg L^{-1}. Therefore, a comparison between the Unilux-measured (in-vivo fluorescence) chlorophyll *a* and HPLC-derived extracted chlorophyll *a* concentrations was undertaken using bulk samples. This yielded a

moderate correlation ($r = 0.77$, $p < 0.05$) with a significant intercept of 2.1 μg L^{-1}, indicating the presence of a non-biological signal affecting the Unilux sensor (Supplementary Figure S4). Furthermore, the "background" Unilux measurements for samples with no detectable autotrophs (according to microscopy) was almost always 2 μg L^{-1}. Therefore, it is highly likely that another source of fluorescence – such as mineral autofluorescence – is present in the signal, and so the Unilux readings cannot be used to say that autotrophs were present.

3.2 Factor Analysis

Factor analysis was undertaken to establish the sources and differential behaviour of the nutrients, cells and chlorophyll. All major ion analyses were included in the analyses. To preserve the variance in the entire dataset, all the separate TOP, MID and SUP ICE samples were used, rather than combined values for each stake. The statistical package SPSS identified six factors with Eigen Values > 1, which collectively explained 76% of the total variance in the dataset. However, only the first three factors produced strong loadings (> 0.7) and were thus amenable to interpretation. Table 1 shows these three factors, highlighting the variables with either strong or moderate loadings (between 0.4 and 0.69) in each case. The first Factor (F1) showed strong positive loadings in the order Na^+, Mg^{2+}, Cl^-, Ca^{2+}, SO_4^{2-} and NO_3^-. There were also strong or moderate negative loadings from PO_4^{3-} and Si. At first glance, Factor 1 seems to be dominated by marine aerosol. However, ratios of Ca^{2+} to Cl^- (both being strong contributors to Factor 1) were in excess of standard marine water ratios, showing a significant non-sea-salt supply of Ca^{2+} (average 85%: data not shown). Therefore, Factor 1 most likely reflects the leaching (elution) of solute from the snowpack, which is dominated by (but is not exclusive to) solute derived from marine aerosol. The strong or moderate negative loadings of PO_4^{3-} and Si respectively were unexpected, but might indicate a different source that became more apparent as the elution of mobile ions progressed.
The second Factor (F2) explained 16% of the variance in the dataset, and was dominated by moderate to strong loadings for DOC, total cell abundance and chlorophyll *a* (0.61, 0.72 and 0.69). It is tempting to suggest that photosynthetic microbes such as cyanobacteria might be responsible for the presence of all three of these variables, but no significant loading was observed with the autotrophic cell abundance due to their absence in the snow. Instead, it seems more likely that Factor 2 represents similar behaviour of bacterial cells, DOC and small, autofluorescent mineral particles that perhaps cause variations in the background chlorophyll *a* readings. Therefore Factor 2 most likely reflects the mobility of particles in the snow matrix during the summer and their provision of NH_4^+.

Like Ca^{2+}, K^+ showed a strong non-marine contribution (average 91%), yet it loaded strongly onto F3 along with NH_4^+ (0.76 and 0.73, respectively). This is most likely indicative of dust or clay weathering processes, as NH_4^+ and K^+ act as interchangeable cations in clay-mineral lattices, and are easily extractable following adsorption onto dust or clay particles.

Table 1. Factor loading analysis for all samples through the melt season. Moderate loadings (i.e., between 0.4 and 0.69) and strong loadings (i.e., > 0.7) are marked by "*" and "**" respectively.

Parameter	**Factor 1**	**Factor 2**	**Factor 3**
Na^+	0.794**	-0.090	0.074
K^+	0.004	-0.113	0.758**
Mg^{2+}	0.778**	0.265	0.158
Ca^{2+}	0.688**	0.496*	0.228
F^-	0.293	0.081	-0.041
Cl^-	0.769**	-0.286	0.189
NO_3^-	0.610**	-0.473*	-0.211
NH_4	-0.268	-0.277	0.727**
PO_4^{3-}	-0.743**	0.111	0.354
SO_4^{2-}	0.650**	-0.205	-0.108
Si	-0.648**	0.012	0.254
Chlorophyll *a* (Chl)	0.235	0.695**	0.320
Autotrophic cell abundance	0.094	0.213	-0.165
Total cell abundance	-0.200	0.718**	-0.277
Dissolved Organic Carbon (DOC)	0.433*	0.606**	0.403*

3.3 Seasonal bacterial production on Foxfonna

Bacterial cell loading estimates (Figure 3F) were used to estimate the total bacterial biomass on Foxfonna, such that the bacterial production (BP) could be estimated from rate of change in biomass (BM) per unit time. Bacterial production was assumed to be negligible during period T1 on account of there being very little liquid water in the cold snowpack (see Figure 2). Therefore, period T2 was the most suitable period for applying this approach, because changes in cell loading were likely dominated by bacterial production on account of the high-water content and its capillary retention within the snow (Reijmer *et al.*, 2012). The loss or gain of bacterial cells by wind-blown snow transport is also likely to have been suppressed greatly by the high-water content in the older snow, and the lack of fresh snowfall events (hence the negligible change in total SWE during T2 on the ice cap shown in Figure 3A).

Under the assumption that only bacterial growth dominated the bacterial cell loading change during transition period T2, bacterial production in snow and superimposed was estimated thus:

$$\mathrm{BP}^{\mathrm{T2}}_{\mathrm{snow}\pm\mathrm{SI}} = c.\left(\frac{\overline{\mathrm{BM}}^{\text{early july}}_{\mathrm{snow}} - \overline{\mathrm{BM}}^{\mathrm{june}}_{\mathrm{snow}} + \overline{\mathrm{BM}}^{\text{early july}}_{\mathrm{SI}}}{\mathrm{T2}}\right) \quad (1)$$

Where $BP^{T2}_{snow\pm SI}$ is the combined average daily bacterial production during T2 for snow and superimposed ice (mg C m^{-2} d^{-1}), T2 is the transition period duration i.e., 32 days, $\overline{BM}$ is average biomass, estimated from average snow or superimposed ice (SI) cell loading on the ice cap (cells m^{-2}). Note that since no superimposed ice layer existed in June, only its cell content in the early July survey needed to be included in the census. Finally, *c* = carbon content of each cell according to Takacs and Priscu (1998).

The results suggest transition period T2 was marked by an increase in bacterial biomass by an order of magnitude throughout the entire snow/ice layer of 2.4 ± 1.5 x 10^{-5} mg C m^{-2} d^{-1}. Of this, up to 1.0 ± 0.5 x 10^{-5} mg C m^{-2} d^{-1} was stored in SUP ICE (the rest being bacterial cells already present in the snow at the onset of T2). Furthermore, biological production cannot be separated between snow and superimposed ice, because all of the bacteria in the ice could have been washed downwards whilst the superimposed ice was forming.

Although conditions were similar during T3, this transition period was dominated by runoff, as shown by the marked SWE depletion in Figure 2. Therefore, it is important to take into account the loss of cells with this runoff, as indicated below. However, it must be noted that cells lost during runoff are more likely to be bacterial than autotrophic, due to the latter's propensity to form cryoconite aggregates and persist for several years on the glacial surface (Hodson, Cameron, *et al.*, 2010).

$$BP^{T3}_{snow\pm SI} = c.\left(\frac{\overline{\mathrm{BM}}^{\text{late july}}_{\mathrm{snow}} - \overline{\mathrm{BM}}^{\text{early july}}_{\mathrm{snow}} + \overline{\mathrm{BM}}^{\text{late july}}_{\mathrm{SI}} - \overline{\mathrm{BM}}^{\text{early july}}_{\mathrm{SI}} + RU^{T3}_{cells}}{\mathrm{T3}}\right) \quad (2)$$

Where RU^{T3}_{cells} is the runoff flux of cells normalised for ice cap area (i.e., cells m^{-2}) and T3 is the duration of Transition period 3, i.e., 23 days. However, uncertainty in RU_{cells} is such that biological production could not be estimated directly during this period. Daily rates of bacterial production in the snowpack and the superimposed ice during T3 were therefore assumed to be half of that deduced from T2, to account for the depletion of SWE to almost zero during this interval.

The rates of seasonal bacterial production were therefore estimated to be negligible in transition period T1 (due to low free water content within the snow), to be 2.4 ± 1.5 x 10^{-5} mg C m^{-2} d^{-1} during transition period T2 and to be 1.2 ± 0.75 mg C m^{-2} d^{-1} during transition period T3. The near-complete ablation of the snowpack and superimposed ice after this means their contribution to bacterial production would have been negligible, and the ecosystem dominated by biological production upon the glacier surface. The total bacterial production within the snow and superimposed ice for the combined 55 days of T2 and T3 was therefore 153 mg C m^{-2} a^{-1}.

3.4 Spatial variations in nutrient concentrations and cells

"TOP" and "MID" snow samples were compared with the superimposed ice and glacial ice samples ("SUP ICE" and "GL ICE", respectively) with respect to the essential macronutrients NH_4^+ and PO_4^{3-}, due to the unexpected increase in their concentrations revealed by Figure 3 D and E. We found that average NH_4^+ concentrations ranged from 0 to 0.04 mg L^{-1} in the April samples of TOP and MID snow (Supplementary Figure S1). However, after the onset of melt and superimposed ice formation, greater average NH_4^+ concentrations (0.05 ± 0.05 mg L^{-1}) appeared in SUP ICE than in the TOP and MID snows (0.03 ± 0.01 and 0.04 ± 0.03 mg L^{-1}, respectively). Concentrations in GL ICE were higher still, but more variable (average 0.07 ± 0.1 mg L^{-1} in early July). The variability was caused by high values at Stake SE (Data Not Shown): a site notable for a high concentration of surface debris. Average PO_4^{3-} concentrations were an order of magnitude lower than NH_4^+ in April and June i.e., from 0.003 to 0.005 mg L^{-1} in TOP and MID snows (Supplementary Figure S1). No PO_4^{3-} was detected in the top layer at stake S1. However, these concentrations increased in early July and ranged from 0.02 - 0.03 mg L^{-1} in TOP and MID snows. SUP ICE exhibited similar concentrations (average 0.03 ± 0.007 mg L^{-1}).

Table 2 shows autotrophic (snow algae and cyanobacteria) and bacterial concentrations (in cells mL^{-1}) identified through bright-field and epifluorescence microscopy. Average cells mL^{-1} are given for all snow (TOP and MID combined), SUP ICE and GL ICE. The average autotrophic cell abundance on the ice cap through the melt season was 0.5 ± 2.7 cells mL^{-1}. The large standard deviation throughout the dataset indicates high spatial variability. All the autotrophic cells in April snow were identified as cyanobacteria, of which 68% were found on the southern and uppermost part of the ice cap (Stakes S1, SW and AWS). Surprisingly, no significant numbers of autotrophic cells were identified in snow for June, early July or late July. No significant numbers of autotrophic cells were observed in superimposed ice either. The only changes in average autotrophic cell abundance were identified from early to late July due to increases in cyanobacteria (e.g., 0.1 ± 0.4 to 2 ± 4 cells mL^{-1} in GL ICE) and also snow algae (e.g., 0.04 ± 0.1 to 0.3 ± 0.5 cells mL^{-1} in SUP ICE). However, snow algal cells were so few and dispersed that their average number on the ice cap often resulted in an unusable value (~ 0 cells mL^{-1}). By contrast, the average bacterial abundance on the ice cap was far greater and increased by an order of magnitude from ca. 10^2 cell mL^{-1} to almost 10^3 cells mL^{-1}. Table 2 shows that changes in the bacterial cell abundance of SUP ICE and GL ICE were more muted than changes in the total snowpack bacterial cell abundance. It also shows that both bacteria and autotrophic cell abundance decreased between April and June. However, the decrease is an artefact of two highly concentrated samples at Stake N that were encountered in April (data not shown). Spatial variability is therefore a major characteristic of the cell distribution across the ice cap, and we could discern no clear patterns underlying this variability, either from stake to stake, or amongst the different sample types.

Table 2. Average cell abundance on Foxfonna. Values are average ± standard deviation.

Sample type	Month	Snow algae (cells mL^{-1})	Cyanobacteria (cells mL^{-1})	Bacteria (cells mL^{-1})
All Snow	April	0	5 ± 9	81 ± 124
	June	0	0	39 ± 19
	Early July	0.2 ± 0.4	0	363 ± 595
	Late July	0.1 ± 0.3	0.7 ± 1.5	935 ± 1460
SUP ICE	Early July	0.04 ± 0.1	0	299 ± 306
	Late July	0.3 ± 0.5	0.1 ± 0.4	185 ± 0
GL ICE	Early July	0.5 ± 0.7	0.1 ± 0.4	565 ± 575
	Late July	0.3 ± 0.6	2 ± 4	818 ± 792

4 Discussion

4.1 Nutrient sources and their non-conservative behaviour in the snowpack

Despite being largely associated with long-range atmospheric pollution (Kühnel *et al.*, 2013), NO_3^- showed a strong, positive loading onto Factor 1 that was similar to that of Cl^-, a biogeochemically conservative ion associated with marine aerosol. Therefore, NO_3^- co-eluted with Cl^- and seems to have been largely conservative during meltwater export (e.g. Tranter and Jones, 2001). By contrast, Figure 3 shows that, NH_4^+ and PO_4^{3-} demonstrated a marked increase in abundance during July, resulting in either a negative loading onto Factor 1 (PO_4^{3-}) or loading onto the separate Factor 3 (NH_4^+). Thereafter, both NH_4^+ and PO_4^{3-} demonstrated an equally marked decrease during July (period T3), which seems to be caused entirely by the rapid ablation of the snowpack. Since the initial, sharp increase in NH_4^+ and PO_4^{3-} coincided with period T2, when liquid water availability rose markedly within the snow matrix, we invoke a dissolution process involving wind-deposited clay and dust particles as the cause.

Dust deposition onto Foxfonna is well known due to the exposure of the desiccated Adventdalen river bed prior to early summer inundation by meltwater (as well as afterwards in early winter). Therefore, it is likely local dust deposited at the surface (early summer) and the base (early winter) of the 2015/16 snowpack was available for dissolution. Interestingly, the apparent conservative behaviour of NO_3^- during the same period provided no evidence for oxidation of the NH_4^+ to NO_3^-, as has been proposed in dry winter snowpacks by Amoroso et al., (2010). However, conversion of NH_4^+ to NO_3^- is readily observed when snowmelt passes through environments that offer greater rock-water contact than the snowpack, such as those at the margins of glaciers (e.g. Hodson *et al.*, 2010). NO_3^- therefore seems to demonstrate largely conservative behaviour when residence times are reduced following the onset of melting conditions during summer.

In summary, local dust-derived sources of NH_4^+ and PO_4^{3-} appear to have combined with long range (marine and anthropogenic aerosol) sources responsible for NO_3^- to deliver critical macro-nutrients to the Foxfonna snowpack during 2015/16.

4.2 No utilization of nutrients by autotrophic communities

The present study demonstrated nutrient behaviour not shown by biologically active snowpacks elsewhere, because the NH_4^+ and PO_4^{3-} released by weathering processes during T2 were not sequestered for autotrophic growth and activity. The acquisition of macronutrients such as NH_4^+, NO_3^- and PO_4^{3-} from rock debris and marine fauna in Antarctica are well known to stimulate autotrophic growth in nutrient-limited snowpacks (Fujii et al., 2010; Hodson et al., 2017). For example, in coastal snowpacks of Livingston Island, Antarctica, the removal of NH_4^+ and PO_4^{3-} from the snow correlated with increasing chlorophyll *a* concentrations that were significantly greater than those reported at Foxfonna. Therefore utilisation of these nutrients by the resident autotrophic communities was a dominant feature of the Livingston Island data set (Hodson et al., 2017b). By contrast, their removal by primary production is conspicuous by its absence in the Foxfonna data.

Nutrients that have yet to be considered could have been responsible for limiting algal growth, such as dissolved inorganic carbon or Fe (Hamilton and Havig, 2017). However, the local geology of Adventdalen valley is dominated by sandstones, siltstones and shales (Rutter et al., 2011) – whose dust deposition within the snow offers DIC and Fe from a range of minerals through natural weathering processes (see Hodson et al., 2017a). Therefore, nutrient limitation seems to be an unlikely explanation for the lack of autotrophic growth on Foxfonna during the study period. Furthermore, a recent study did encounter a significant population of red snow algae and ice algae in snow and ice samples on Foxfonna (Fiołka *et al.*, 2021). This study was conducted in late August in 2011, and suggests, in accordance with the authors' own observations throughout 15 years of mass balance survey, that there is marked annual variability in snow algae population dynamics.

An important environmental factor is likely to have been the role that the heterogeneity of the snowpack plays in governing how conducive it becomes for autotroph proliferation, especially since a great many would be expected to reside on the glacier surface prior to the onset of snowmelt (Stibal *et al.*, 2015). For example, the nutrient resource available within the snowpack layers (Figure 3**)** would have presented an excellent opportunity for flagellated vegetative forms of green algal cells to make their way upwards towards the snow surface, seeking light and nutrients (Stibal *et al.*, 2007). However, their motility from the glacier surface through the snowpack was most likely impeded by the refrozen superimposed ice layer and other ice lenses that formed during transition period T2.

Given the above, the most important limitation to the autotrophic production seems to be insufficient inocula of snow algal cells within the fresh winter snowpack (and potentially upon the previous summer surface) to allow germination of new cells (Hoham et al., 2006). Therefore, it is proposed that the sustained, low autotrophic cell abundance is most likely caused by the high elevation of Foxfonna and its sustained negative mass balance, which is responsible for the removal of all snow from the summit of the ice cap, leaving no residual firn to provide inocula to meltwaters percolating down through the system. Secondly, the community typically has only a short opportunity to respond to the increase in energy and nutrients during summer (55 days) before biomass is removed by further ablation. Finally, since the environment under study is by no means unique, the likely response of the snowpack autotrophic community in other high elevation polar ice caps might also be restricted in this way, suggesting that many will be dominated by bacterial production as they lose their perennial snow covers.

4.3 Assessing the importance of bacterial carbon production on Foxfonna

Significant changes in carbon resources were detectable during T2 because bacterial cell abundance increased from 39 ± 19 to 363 ± 595 cells mL^{-1} (Table 2). These bacterial cell numbers are more representative of Antarctic snows (Carpenter, Lin and Capone, 2000; Michaud et al., 2014) than the Arctic or Alpine snows (Amato et al., 2007) and were used to estimate bacterial production during transition periods T2 and T3 was ca. 153 mg C m^{-2} a^{-1} (Section 3.2). For these calculations, a fixed bacterial carbon content per cell (11 fg C $cell^{-1}$) was employed based on prior work on carbon reservoirs in polar habitats (Kepner et al., 1998, Takacs and Priscu, 1998, Priscu et al., 2008). This value of 11 fg C $cell^{-1}$ had been previously used: 1) to calculate carbon released from microbial populations via viral lysis in Antarctic lakes (Kepner, Wharton and Suttle, 1998), 2) to understand the bacterioplankton dynamics in permanently ice-covered lakes in the McMurdo Dry Valleys, Antarctica (Takacs and Priscu, 1998), and most importantly, 3) to estimate prokaryotic cellular carbon reservoir in all Antarctic habitats, namely, lakes, subglacial aquifers and the ice sheets (Priscu et al., 2008). These estimates, although published in 2008, did not use any of the available allometric and linear volume-to-carbon conversion factors. These factors, compiled by Posch et al. (2001), were, however used by Bellas et al. (2013) to estimate a range for bacterial carbon production in Arctic cryoconite sediments.

Irvine-Fynn et al. (2012) quantified cell budgets on an Arctic glacier surface using flow cytometry, compared both cell-to-carbon and volume-to-carbon conversions, but opted for the higher value of 20 fg C $cell^{-1}$ (from Whitman, Coleman and Wiebe, 1998), to estimate annual carbon export from a supraglacial catchment on Midtre Lovénbreen (Svalbard). In their study, the cell abundance, size and shape were enumerated through flow cytometry, classified on the basis of size. With the greatest proportion of cells being ≤ 3 μm, they were presumed to be spherical-shaped heterotrophic bacteria. It is also interesting to note that the value of 20 fg C $cell^{-1}$ applied for heterotrophic cell carbon production by these authors, has also been used to estimate autotrophic snow algal carbon production in several Arctic/Antarctic carbon estimation studies (e.g. Fogg, 1967; Takeuchi et al., 2006). On the other hand, for their allometric volume-to-carbon estimation, wherein spherical shaped cells were assumed, the formula given by Felip et al. (2007) was applied:

$$CC = 120\, x\, V^{0.72} \quad (3)$$

Where CC is the carbon content (fg C $cell^{-1}$) and V is the biovolume (μm^3).

This formula, however, was used for rod-shaped bacteria to study bacterial biomass in mountain lakes (Felip et al., 2007), and earlier to estimate biomass in the snow and ice covers of such lakes (Felip et al., 1995). This allometric model was originally given by Norland et al. (1993), where the geometric shape of the bacteria was approximated as a cylinder with hemispherical ends, based on electron microscopy and X-ray analysis of bacterial cultures. It is unclear whether the carbon content formula stays relevant for spherical bacterial cells or was intended to be used only for rod-shaped cells. This shows that differences in methods for volume estimation and the carbon content, can introduce significant variability in the carbon budget estimations and therefore the need arises to have a consensus and a standard on the parameters that are to be used for such estimations.

The summary of conversion factors from (Posch et al., 2001) incorporates different size range, habitat, preparation techniques and growth conditions, but would have benefited from inclusion of a column listing the method for volume estimation involved in each of the referenced methods. Therefore, the worker needs to be careful and take into account the different parameters being used during selection of the appropriate model for their use. It might not be possible to reach a worldwide consensus on carbon estimation protocols yet, but it is important that a laboratory group produce repeatable estimations following a standard protocol so that they may be comparable and significant errors can be avoided.

Table 3. Cell-to-carbon and volume-to-carbon bacterial carbon production values during T2 (June – early July) on Foxfonna.

Sampling Survey (Transition period)	**Estimated areal bacterial production (mg C m^{-2} day^{-1}) in snow**
Cell-to-carbon	*$2.4 \times 10^{-5} \pm 4 \times 10^{-5}$
	¹$4.3 \times 10^{-5} \pm 7.3 \times 10^{-5}$
Allometric C-per-cell	˜1.2 ± 2
	ˠ1.9 ± 3.2

Note: Cellular carbon content *11 fg C $cell^{-1}$ (Takacs and Priscu, 1998), ¹20 fg C $cell^{-1}$ (Whitman, Coleman and Wiebe, 1998),˜ assumes allometric C-per-cell from *(Felip et al., 2007) and ˠ(Posch et al., 2001)

For comparison purposes, Table 4 compiles bacterial carbon production numbers on a daily basis for all cell-to-carbon and volume-to-carbon conversions calculations discussed above. For obvious reasons, using 20 fg C $cell^{-1}$ instead of 11 fg C $cell^{-1}$ results in a bacterial carbon production value which is nearly double (e.g., for snow: $2.4 \times 10^{-5} \pm 4 \times 10^{-5}$ mg C m^{-2} day^{-1} and $4.3 \times 10^{-5} \pm 7.3 \times 10^{-5}$ mg C m^{-2} day^{-1}). In contrast, the cell-to-volume allometric conversions are ~ 5 orders of magnitude higher (1.2 ± 2 mg C m^{-2} day^{-1} and 1.9 ± 3.2 mg C m^{-2} day^{-1}). This shows that the use of these two different approaches can introduce significant uncertainty in the carbon budget and there needs to be both a standardisation of techniques and a consensus as to which conversion approach should be employed. The range of results here makes comparison with other studies difficult. For example, the bacterial carbon production values for two glacial snowpacks in the maritime Antarctic (Signy island) that were deduced using radiolabel incorporation experiments were significantly higher than in this study (11 ± 12 and 17 ± 11 mg C m^{-2} d^{-1}), but the difference can to some extent be attributed to the higher bacterial cell abundance at Signy (10^3 -10^4 cells mL^{-1} as opposed to 10^2 - 10^3 cells mL^{-1} in this study). With this being the case, the allometric conversions seem most appropriate.

The tendency for net heterotrophy is not in agreement with studies of glacier surface (e.g., Tedstone et al., 2017; Williamson et al., 2018, 2020; Cook et al., 2020) and low elevation snowpacks, such as those in the maritime Antarctic (e.g., Gray et al., 2020). However, it is likely that time, more persistent snow cover and nutrient abundance are the key factors limiting the development of autotrophic biomass in the system under study. Furthermore, the snowpack lacked a sufficient autotrophic biomass to start with, with there being virtually none of the so-called snow algae and only modest abundance of cyanobacteria capable of photosynthesis.

5 Conclusions

The present study has been one of the first attempts to thoroughly examine a glacial snowpack ecosystem with respect to its seasonal thermal, biogeochemical and microbial community evolution. The mass balance nutrient data revealed that NH_4^+ and PO_4^{3-}, both essential for biological processes, displayed a non-conservative behaviour (as opposed to Cl^- and NO_3^-), i.e., they did not follow the expected elution dynamics for a melting snowpack. However, this was not due to sequestration by autotrophic communities, but dust fertilisation and weathering processes that supplemented the winter atmospheric bulk deposition on the ice cap. Indeed, the average autotrophic abundance on the ice cap throughout the melt season was just 0.5 ± 2.7 cells mL^{-1}. Therefore, the total seasonal biological production within the combined layers of snow and superimposed ice was dominated by bacteria, allometrically estimated at 153 mg C m^{-2}, resulting in a net-heterotrophic (bacterial) snowpack ecosystem. Superimposed ice possessed the same chemical and biological features as the overlying snow, and the percolation of meltwater through the snowpack did not result in any enrichment of nutrients or cells. For the same reason, biological production within the superimposed ice could not be separated from production within the snow. Thus, superimposed ice played a passive role, acting as a temporary dilute storage for nutrients and cells and an effective barrier between the snow and the debris- and cell-rich glacier ice that lay beneath. Bacterial production rates were compared between linear and allometric models of carbon estimation. The latter compared most favourably with studies from the maritime Antarctic and lay in the range 1.2 ± 2 to 1.9 ± 3.2 mg C m^{-2} day^{-1}. However, since autotrophic cells are so much larger than bacterial cells, carbon budgets will be greatly influenced by summers when snow algae are more successful. However, since glacial snowpacks will disappear sooner in a warming climate, they are more likely to be largely net-heterotrophic bacterial ecosystems than autotrophic ecosystems. This is important because fewer nutrients will be assimilated within the snow under these circumstances, and so more will be exported to downstream aquatic ecosystems during early summer.

6 Acknowledgements

The author thanks the Commonwealth Scholarship Commission (CSC) for funding through a CSC PhD Scholarship (INCS-2015-214) and the Research Council of Norway BIOICE project (Grant Number 288402). We thank the University Centre in Svalbard (UNIS) students and logistics for their help and support during field work. Imaging work was performed at the Wolfson Light Microscopy Facility (LMF), University of Sheffield under the guidance of Dr. Darren Robinson. Dr. Chris Williamson is thanked for HPLC analysis on the samples.

7 References

Amato, P. *et al.* (2007) 'Bacterial characterization of the snow cover at Spitzberg, Svalbard', *FEMS Microbiology Ecology*, 59(2), pp. 255–264. doi:10.1111/j.1574-6941.2006.00198.x.

Amoroso, A. *et al.* (2010) 'Microorganisms in dry polar snow are involved in the exchanges of reactive nitrogen species with the atmosphere', *Environmental Science and Technology*, 44(2), pp. 714–719. doi:10.1021/es9027309.

Barbesti, S. *et al.* (2000) 'Two and three-color fluorescence flow cytometric analysis of immunoidentified viable bacteria', *Cytometry*, 40(3), pp. 214–218. doi:10.1002/1097-0320(20000701)40:3<214::AID-CYTO6>3.0.CO;2-M.

Bellas, C.M. *et al.* (2013) 'Viral impacts on bacterial communities in Arctic cryoconite', *Environmental Research Letters*, 8(4). doi:10.1088/1748-9326/8/4/045021.

Carpenter, E.J., Lin, S. and Capone, D.G. (2000) 'Bacterial Activity in South Pole Snow', *Applied and Environmental Microbiology*, 66(10), pp. 4514–4517. doi:10.1128/AEM.66.10.4514-4517.2000.

Cook, J.M. *et al.* (2020) 'Glacier algae accelerate melt rates on the south-western Greenland Ice Sheet', *Cryosphere*, 14(1). doi:10.5194/tc-14-309-2020.

Cook, Joseph M. *et al.* (2020) 'Glacier algae accelerate melt rates on the western Greenland Ice Sheet', *The Cryosphere Discussions*, 14(1), pp. 1–31. doi:10.5194/tc-2019-58.

Felip, M. *et al.* (1995) *Highly Active Microbial Communities in the Ice and Snow Cover of High Mountain Lakes*, *Applied and Environmental Microbiology*. Available at: http://aem.asm.org/ (Accessed: 25 September 2018).

Felip, M. *et al.* (2007) 'Suitability of flow cytometry for estimating bacterial biovolume in natural plankton samples: Comparison with microscopy data', *Applied and Environmental Microbiology*, 73(14), pp. 4508–4514. doi:10.1128/AEM.00733-07.

Fiołka, M.J. *et al.* (2021) 'Morphological and spectroscopic analysis of snow and glacier algae and their parasitic fungi on different glaciers of Svalbard', *Scientific Reports*, 11(1), p. 21785. doi:10.1038/s41598-021-01211-8.

Fogg, G.. (1967) 'Observations on the Snow Algae of the South Orkney Islands', *Philosophical Transactions of the Royal Society of London*, 252(777), pp. 279–287.

Fujii, M. *et al.* (2010) 'Microbial community structure, pigment composition, and nitrogen source of red snow in antarctica', *Microbial Ecology*, 59(3), pp. 466–475. doi:10.1007/s00248-009-9594-9.

Gray, A. *et al.* (2020) 'Remote sensing reveals Antarctic green snow algae as important terrestrial carbon sink', *Nature Communications*, 11, p. 2527. doi:10.1038/s41467-020-16018-w.

Grégori, G. *et al.* (2001) 'Resolution of Viable and Membrane-Compromised Bacteria in Freshwater and Marine Waters Based on Analytical Flow Cytometry and Nucleic Acid Double Staining', *Applied and Environmental Microbiology*, 67(10), pp. 4662–4670. doi:10.1128/AEM.67.10.4662-4670.2001.

Hamilton, T.L. and Havig, J. (2017) 'Primary productivity of snow algae communities on stratovolcanoes of the Pacific Northwest', *Geobiology*, 15(2), pp. 280–295. doi:10.1111/gbi.12219.

Hodson, A., Roberts, T.J., *et al.* (2010) 'Glacier ecosystem response to episodic nitrogen enrichment in Svalbard, European High Arctic', *Biogeochemistry*, 98(1–3), pp. 171–184.

doi:10.1007/s10533-009-9384-y.
Hodson, A., Cameron, K., *et al.* (2010) 'The structure , biological activity and biogeochemistry of cryoconite aggregates upon an Arctic valley glacier : Longyearbreen , Svalbard', *Journal of Glaciology*, 56(196), pp. 349–362.
Hodson, Andy *et al.* (2017) 'Climatically sensitive transfer of iron to maritime Antarctic ecosystems by surface runoff', *Nature Communications*, 8, pp. 1–7. doi:10.1038/ncomms14499.
Hodson, Andrew *et al.* (2017) 'Microbes influence the biogeochemical and optical properties of maritime Antarctic snow', *Journal of Geophysical Research: Biogeosciences*, 122(6), pp. 1456–1470. doi:10.1002/2016JG003694.
Hoham, R.W. *et al.* (2006) 'Two new species of green snow algae from Upstate New York, Chloromonas chenangoensis sp. nov. and Chloromonas tughillensis sp. nov. (Volvocales, Chlorophyceae) and the effects of light on their life cycle development', *Phycologia*, 45(3), pp. 319–330. doi:10.2216/04-103.1.
Irvine-Fynn, T.D.L. *et al.* (2012) 'Microbial cell budgets of an Arctic glacier surface quantified using flow cytometry', *Environmental Microbiology*, 14(11), pp. 2998–3012. doi:10.1111/j.1462-2920.2012.02876.x.
Kepner, R.L., Wharton, R.A. and Suttle, C.A. (1998) 'Viruses in Antarctic lakes.', *Limnology and oceanography*, 43(7), pp. 1754–1761. doi:10.4319/lo.1998.43.7.1754.
Krug, L. *et al.* (2020) 'The microbiome of alpine snow algae shows a speci fi c inter-kingdom connectivity and algae-bacteria interactions with supportive capacities', *The ISME Journal* [Preprint]. doi:10.1038/s41396-020-0677-4.
Kühnel, R. *et al.* (2013) 'Reactive nitrogen and sulphate wet deposition at Zeppelin Station, Ny-Ålesund, Svalbard', *Polar Research*, 32. doi:10.3402/polar.v32i0.19136.
Lebaron, P., Parthuisot, N. and Catala, P. (1988) 'Comparison of blue nucleica cid dyes for the flow cytometry enumeration of bacteria in aquatic systems.', *Applied and Environmental Microbiology*, 64(5), pp. 1724–1730. doi: .
Michaud, L. *et al.* (2014) 'Snow surface microbiome on the High Antarctic Plateau (DOME C).', *PLoS ONES ONE*, 9(8), p. e104505. doi:10.1371/journal.pone.0104505.
Mikucki, J.A. and Priscu, J.C. (2007) 'Bacterial diversity associated with blood falls, a subglacial outflow from the Taylor Glacier, Antarctica', *Applied and Environmental Microbiology*, 73(12), pp. 4029–4039. doi:10.1128/AEM.01396-06.
Nowak, A., Hodson, A. and Turchyn, A. V. (2018) 'Spatial and Temporal Dynamics of Dissolved Organic Carbon, Chlorophyll, Nutrients, and Trace Metals in Maritime Antarctic Snow and Snowmelt', *Frontiers in Earth Science*, 6, p. 201. doi:10.3389/feart.2018.00201.
P. Kemp, B. F. Sherr, E. B. Sherr, and J.J.C. (1993) 'The relation between biomass and volume of bacteria', in *Handbook of Methods in Aquatic Microbiology*, pp. 303–308. Available at: https://books.google.co.uk/books?hl=en&lr=&id=ql1ZDwAAQBAJ&oi=fnd&pg=RA1-PA35&dq=Norland,+S.+1993.+The+relationship+between+biomass+and+volume+of+bacteria,+p.+303–307.+In+P.+F.+Kemp,+B.+F.+Sherr,+E.+B.+Sherr,+and+J.+J.+Cole+(ed.),+Handbook+of+methods+in+a.
Posch, T. *et al.* (2001) 'Precision of bacterioplankton biomass determination: A comparison of two fluorescent dyes, and of allometric and linear volume-to-carbon

conversion factors', *Aquatic Microbial Ecology*, 25(1), pp. 55–63. doi:10.3354/ame025055.

Reijmer, C.H. *et al.* (2012) 'Refreezing on the Greenland ice sheet: A comparison of parameterizations', *The Cryosphere*, 6(4), pp. 743–762. doi:10.5194/tc-6-743-2012.

Rutter, N. *et al.* (2011) 'Hydrology and hydrochemistry of a deglaciating high-Arctic catchment, Svalbard', *Journal of Hydrology*, 410(1–2), pp. 39–50. doi:10.1016/j.jhydrol.2011.09.001.

Skidmore, M.L., Foght, J.M. and Sharp, M.J. (2000) 'Microbial life beneath a high Arctic glacier', *Applied and Environmental Microbiology*, 66(8), pp. 3214–3220. doi:10.1128/AEM.66.8.3214-3220.2000.

Stibal, M. *et al.* (2007) 'Seasonal and diel changes in photosynthetic activity of the snow alga Chlamydomonas nivalis (Chlorophyceae) from Svalbard determined by pulse amplitude modulation fluorometry', *FEMS Microbiology Ecology*, 59(2), pp. 265–273. doi:10.1111/j.1574-6941.2006.00264.x.

Stibal, M. *et al.* (2015) 'Microbial abundance in surface ice on the Greenland Ice Sheet.', *Frontiers in Microbiology*, 6(March), p. 225. doi:10.3389/fmicb.2015.00225.

Takacs, C.D. and Priscu, J.C. (1998) 'Bacterioplankton dynamics in the McMurdo Dry Valley lakes, Antarctica: Production and biomass loss over four seasons', *Microbial Ecology*, 36(3), pp. 239–250. doi:10.1007/s002489900111.

Takeuchi, N. *et al.* (2006) 'Spatial distribution and abundance of red snow algae on the Harding Icefield, Alaska derived from a satellite image', *Geophysical Research Letters*, 33(21), pp. 1–6. doi:10.1029/2006GL027819.

Tedstone, A.J. *et al.* (2017) 'Dark ice dynamics of the south-west Greenland Ice Sheet', *The Cryosphere*, 11(6), pp. 2491–2506. doi:10.5194/tc-11-2491-2017.

Tranter, M. and Jones, H.G. (2001) 'The Chemistry of Snow: Processes and Nutrient Cycling', *Snow ecology: An Interdisciplinary Examination of Snow-Covered Ecosystems*, 22(6), pp. 127–167.

Whitman, W.B., Coleman, D.C. and Wiebe, W.J. (1998) 'Prokaryotes: The unseen majority', *Proceedings of the National Academy of Sciences*, 95(12), pp. 6578–6583. doi:10.1073/pnas.95.12.6578.

Williamson, C.J. *et al.* (2018) 'Ice algal bloom development on the surface of the Greenland Ice Sheet', *FEMS Microbiology Ecology*, 94(3). doi:10.1093/femsec/fiy025.

Williamson, C.J. *et al.* (2020) 'Algal photophysiology drives darkening and melt of the Greenland Ice Sheet', *Proceedings of the National Academy of Sciences*, pp. 1–12. doi:10.1073/pnas.1918412117.

JGR Biogeosciences

Supporting Information for

Seasonal snowpack microbial ecology and biogeochemistry on a High Arctic ice cap reveals negligible autotrophic activity during spring and summer melt

A. Dayal[1], A.J. Hodson[2,3], M. Šabacká[4] and A. L. Smalley[5]

[1]Institute of Biological, Environmental & Rural Sciences, Aberystwyth University, Aberystwyth, UK. [2]Arctic Geology Department, University Centre in Svalbard, Longyearbyen, Norway. [3]Department of Environmental Sciences, Western Norway University of Applied Sciences, Sogndal, Norway. [4]Centre for Polar Ecology, University of South Bohemia, Czech Republic. [5]Department of Geography, University of Sheffield, UK.

Contents of this file

Introduction

Text S1.

For the allometric conversions (Table 4) , i.e. between carbon and volume with a scaling factor, one model each was chosen from Felip et al. (2007) which employed carbon estimates for freshwater bacteria and Posch et al. (2001). The allometric carbon calculations were as follows:

$$C = 120\, x\, V^{0.72} \text{ (Felip et al., 2007)} \quad (4)$$

Where, C is the carbon content (pg C cell^{-1})
V is the mean biovolume of the cell (μm^3)

In this case, the mean bacterial biovolume in snow and superimposed ice and glacial ice for T2 (June – Early July) are 8.3 μm^3 and 59.4 μm^3.

Briefly, the total biovolume for each sampled snow layer per stake was calculated. The combined average of all the sampled snow layers for each stake gave the mean bacterial volume used in the formulae below:

Equations 1 and 2 were then modified to estimate bacterial carbon production where the Bacterial Carbon Content (BCC; 11 fg C cell^{-1}) is replaced by 551 x 10^3 fg C cell^{-1}, 2271 x 10^3 fg C cell^{-1} and 1718 x 10^3 fg C cell^{-1}, respectively. This results in the numbers presented below.

$$C_{snow} = 120\ x\ 8.3^{0.72} = 551\ pg\ C\ cell^{-1} = 551\ x\ 10^3\ fg\ C\ cell^{-1} \quad (5)$$

$$C_{sup\ ice} = 120\ x\ 59.4^{0.72} = 2271\ pg\ C\ cell^{-1} = 2271\ x\ 10^3\ fg\ C\ cell^{-1} \quad (6)$$

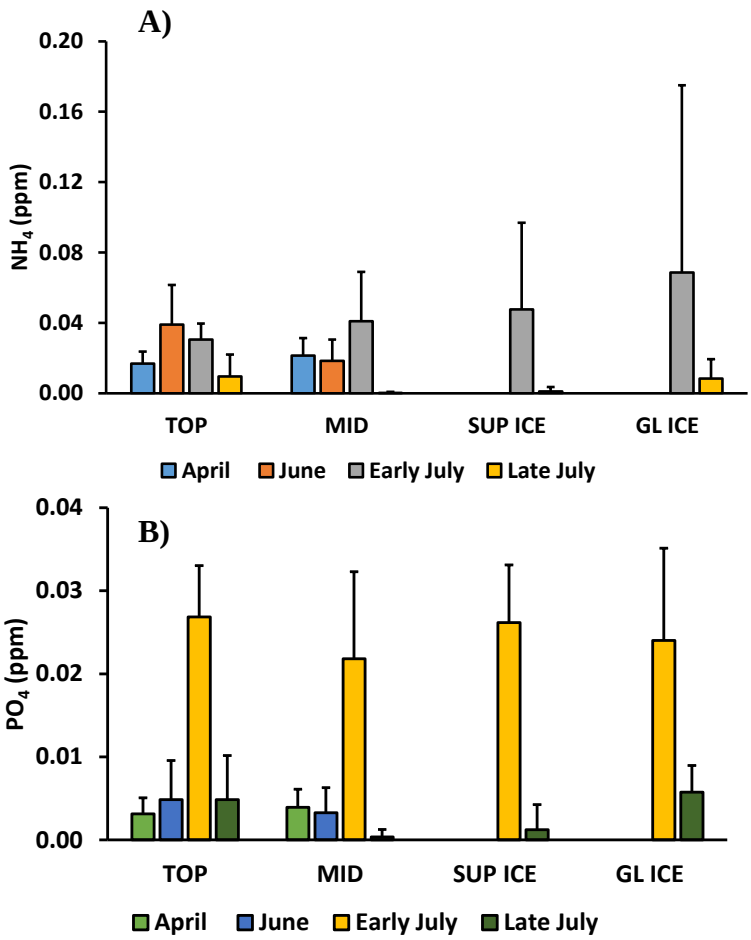

Figure S1. Seasonal and temporal change in NH_4^+ and PO_4^{3-} concentrations (ppm) on Foxfonna.

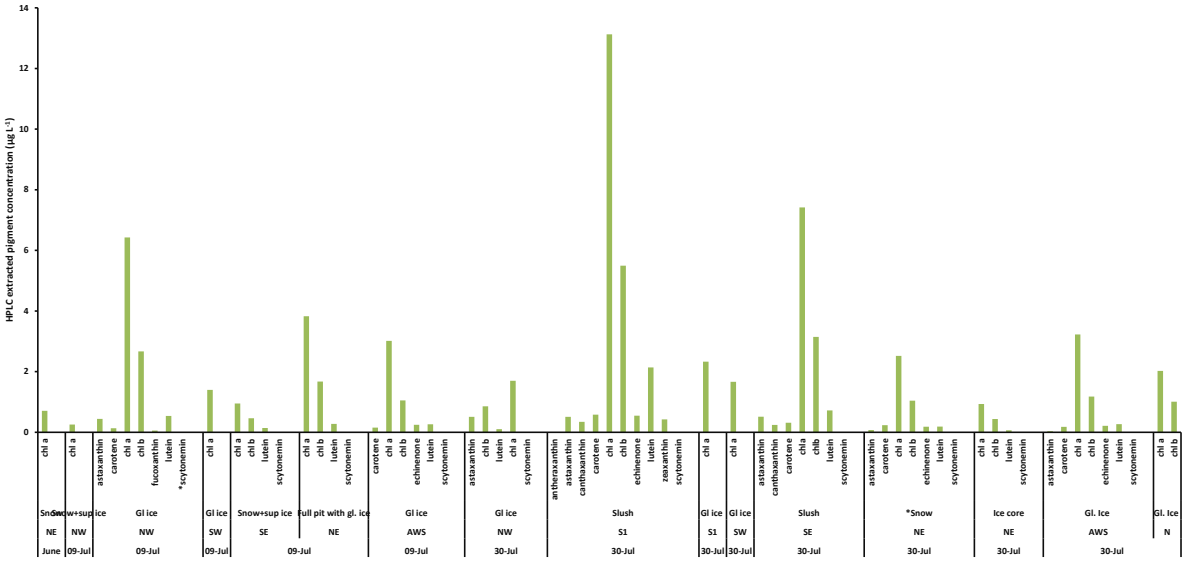

Figure S1. HPLC extracted pigment yield (µg L^{-1}) on Foxfonna.
Note: Out of the 42 samples analysed, 26 had no measurable pigment concentrations. However, an internal standard for checking the effectiveness of the extraction as well as pigment standards returned good results.

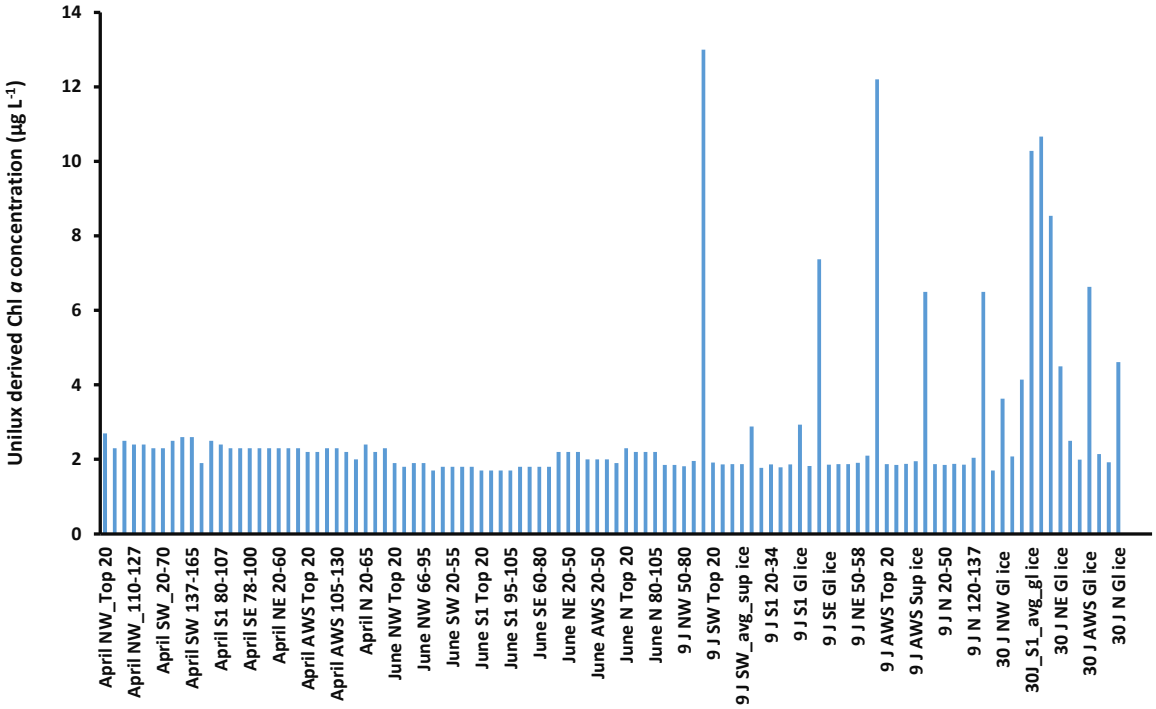

Figure S2. Unilux derived Chl *a* concentration changes through the melt season on Foxfonna.

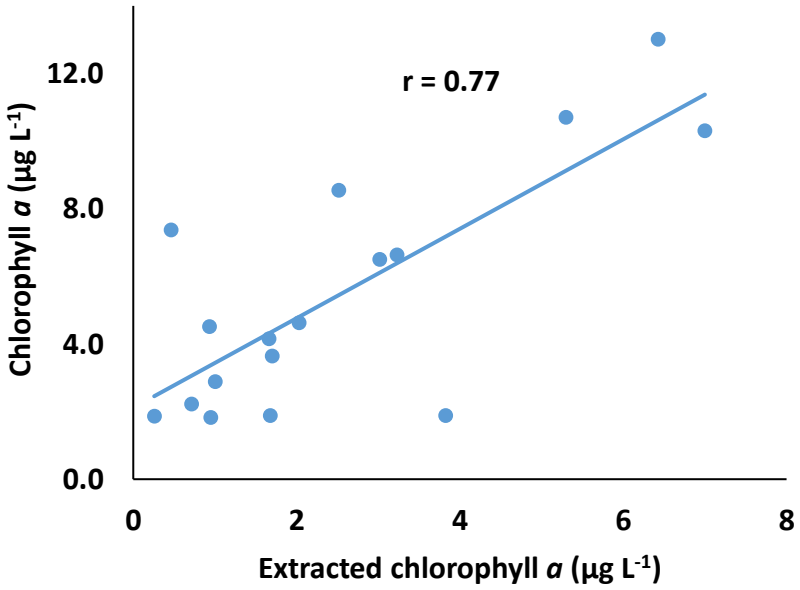

Figure S3. Correlation between extracted and Unilux measured chlorophyll *a* concentrations (µg L^{-1}).

Table S1. Concentrations of cations Na^+, K^+, Mg^{2+}, Ca^{2+}, anions F^-, SO_4^{2-}, Si and DOC in ppm for each sample in April.

Sample	Na^+	K^+	Mg^{2+}	Ca^{2+}	F^-	SO_4^{2-}	Si	DOC
April NW Top 20	0.86	0.07	0.27	0.40	0.24	0.45	0.01	0.44
April NW 20-72	1.18	0.08	0.19	0.31	0.05	0.56	0.00	0.35
April NW 72-110	0.57	0.06	0.10	0.38	n.a.	0.12	0.01	0.61
April NW110-127	1.59	0.11	0.23	0.35	n.a.	0.00	0.00	0.38
April NW 127-165	1.00	0.14	0.17	0.35	n.a.	0.50	0.00	0.39
April SW Top 20	0.85	0.07	0.15	0.35	n.a.	0.34	0.00	0.30
April SW 20-70	1.13	0.06	0.21	0.26	n.a.	0.63	0.00	0.29
April SW 70-100	0.92	0.07	0.16	0.33	0.17	0.35	0.00	0.98
April SW 100-137	1.48	0.20	0.20	0.45	0.10	0.54	0.00	0.95
April SW 137-165	1.33	0.13	0.19	0.31	0.03	0.72	0.00	0.76
April S1 Top 20	0.78	0.06	0.16	0.41	0.02	0.47	0.00	0.29
April S1 20-80	1.11	0.06	0.22	0.32	0.24	0.42	0.00	0.29
April S1 80-107	0.47	0.04	0.11	0.26	n.a.	0.23	0.00	0.26
April SE Top 20	2.41	0.09	0.38	0.62	0.01	0.48	0.00	0.26
April SE 20-78	1.27	0.06	0.24	0.39	0.45	0.35	0.00	0.002
April SE 78-100	0.79	0.05	0.15	0.30	n.a.	0.22	0.00	0.25
April SE 100-126	0.56	0.06	0.12	0.32	0.18	0.20	0.00	0.38
April NE Top 20	1.16	0.07	0.20	0.28	0.26	0.54	0.00	0.18
April NE 20-60	1.02	0.05	0.15	0.20	0.01	0.44	0.00	0.32
April NE 60-98	1.13	0.05	0.21	0.21	n.a.	0.40	0.00	0.17
April NE 98-127	0.49	0.03	0.12	0.16	0.12	0.24	0.00	0.21
April AWS Top 20	0.75	0.06	0.13	0.15	0.03	0.58	0.00	0.27
April AWS 20-75	0.89	0.06	0.13	0.11	0.02	0.62	0.00	0.31
April AWS 75-105	0.82	0.05	0.14	0.14	0.04	0.29	0.00	0.31
April AWS 105-130	0.96	0.08	0.14	0.28	0.02	0.34	0.00	0.36
April AWS 130-168	1.25	0.07	0.15	0.12	0.04	0.55	0.00	0.35
April N Top 20	1.24	0.07	0.18	0.32	0.05	0.51	0.00	0.23
April N 20-65	1.06	0.06	0.19	0.30	0.04	0.61	0.00	0.43
April N 65-90	0.84	0.06	0.17	0.31	0.03	0.31	0.00	
April N 90-100	1.05	0.10	0.15	0.32	0.03	0.45	0.00	0.44

Table S2. Concentrations of cations Na^+, K^+, Mg^{2+}, Ca^{2+}, anions F^-, SO_4^{2-}, Si and DOC in ppm for each sample in June.

Sample	Na^+	K^+	Mg^{2+}	Ca^{2+}	F^-	SO_4^{2-}	Si	DOC
June NW Top 20	0.81	0.11	0.03	0.13	0.15	0.62	0.00	0.25
June NW 20-54	1.24	0.08	0.02	0.32	n.a.	0.55	0.00	0.19
June NW 54-66	0.83	0.03	0.02	0.24	0.02	0.29	0.01	0.25
June NW 66-95	0.84	0.06	0.02	0.26	n.a.	0.32	0.00	0.48
June NW 95-100	2.65	0.03	0.04	0.65	0.02	0.86	0.00	0.52
June SW Top 20	0.65	0.09	0.02	0.14	0.02	0.45	0.00	0.19
June SW 20-55	0.81	0.07	0.02	0.16	0.02	0.64	0.01	0.20
June SW 55-85	1.36	0.04	0.02	0.32	0.02	0.36	0.00	0.14
June SW 85-110	0.84	0.04	0.02	0.20	n.a.	0.40	0.00	0.21
June S1 Top 20	0.72	0.08	0.03	0.14	n.a.	0.65	0.00	0.18
June S1 20-58	1.00	0.03	0.02	0.29	0.01	0.50	0.00	0.14
June S1 58-95	0.79	0.03	0.01	0.24	0.03	0.27	0.01	0.12
June S1 95-105	0.55	0.04	0.13	0.21	n.a.	0.18	0.01	0.25
June SE Top 20	0.51	0.09	0.02	0.13	n.a.	0.48	0.01	0.16
June SE 20-60	0.74	0.05	0.12	0.18	n.a.	0.75	0.01	0.24
June SE 60-80	1.40	0.06	0.25	0.19	n.a.	0.39	0.01	0.14
June SE 80-115	0.24	0.02	0.07	0.23	n.a.	0.17	0.02	0.14
June NE Top 20	0.80	0.02	0.11	0.14	n.a.	0.74	0.02	0.23
June NE 20-50	1.26	0.07	0.19	0.20	n.a.	0.44	0.03	0.16
June NE 50-80	0.95	0.05	0.17	0.13	n.a.	0.40	0.00	0.16
June AWS Top 20	0.68	0.06	0.12	0.19	n.a.	0.50	0.00	0.15
June AWS 20-50	0.76	0.04	0.13	0.14	n.a.	0.47	0.00	0.12
June AWS 50-80	0.82	0.04	0.13	0.12	n.a.	0.39	0.01	0.11
June AWS 80-95	1.18	0.07	0.21	0.18	n.a.	0.33	0.00	0.17
June N Top 20	0.21	0.04	0.02	0.11	n.a.	0.52	0.00	0.15
June N 20-50	0.86	0.05	0.12	0.10	n.a.	0.30	0.01	0.24
June N 50-80	1.24	0.06	0.22	0.17	n.a.	0.53	0.01	0.14
June N 80-105	0.69	0.04	0.15	0.12	n.a.	0.34	0.01	0.15

Table S3. Concentrations of cations Na^+, K^+, Mg^{2+}, Ca^{2+}, anions F^-, SO_4^{2-}, Si and DOC in ppm for each sample in early July.

Sample	Na^+	K^+	Mg^{2+}	Ca^{2+}	F^-	SO_4^{2-}	Si	DOC
9 J NW Top 20	0.82	0.09	0.12	0.16	0.04	0.00	0.00	0.23
9 J NW 20-50	0.50	0.02	0.02	0.19	0.02	0.00	0.03	0.29
9 J NW 50-80	0.49	0.03	0.02	0.16	0.02	0.07	0.03	0.17
9 J NW Sup ice	0.68	0.06	0.07	0.15	0.02	0.09	0.03	0.19
9 J NW Gl ice	0.96	0.06	0.01	0.25	0.01	0.26	0.03	0.62
9 J SW Top 20	0.68	0.00	0.01	0.06	0.02	0.03	0.03	0.39
9 J SW 20-50	0.26	0.07	0.00	0.03	n.a.	0.04	0.03	0.13
9 J SW 50-80	0.38	0.02	0.02	0.11	0.02	0.00	0.03	0.20
9 J SW Sup ice	0.54	0.06	0.05	0.13	0.02	0.00	0.02	0.16
9 J SW Gl ice	1.14	0.03	0.01	0.24	0.04	0.07	0.00	0.30
9 J S1 Top 20	0.24	0.04	0.01	0.03	0.01	0.00	0.00	0.16
9 J S1 20-34	0.26	0.02	0.01	0.02	n.a.	0.03	0.00	0.15
9 J S1 34-40	0.32	0.70	0.01	0.02	0.01	0.00	0.00	0.15
9 J S1 Sup ice	0.33	0.07	0.01	0.05	0.02	0.02	0.00	0.21
9 J S1 Gl ice	0.76	0.12	0.02	0.19	0.02	0.00	0.00	0.21
9 J SE Top 20	0.35	0.11	0.02	0.03	0.02	0.00	0.00	0.17
9 J SE Sup ice	0.95	0.33	0.03	0.22	0.02	0.26	0.00	0.43
9 J SE Gl ice	0.59	0.81	0.03	0.12	0.02	0.15	0.04	0.21
9 J NE Top 20	0.46	0.01	0.01	0.04	0.02	0.00	0.04	0.12
9 J NE 20-50	0.36	0.02	0.01	0.04	0.02	0.00	0.04	0.31
9 J NE 50-58	0.35	0.04	0.05	0.14	0.01	0.06	0.04	0.19
9 J NE Sup ice	0.21	0.06	0.08	0.27	0.01	0.18	0.04	0.15
9 J NE Gl ice	0.83	0.02	0.03	0.21	0.02	0.49	0.04	0.31
9 J AWS Top 20	0.54	0.00	0.01	0.04	0.02	0.00	0.04	0.18
9 J AWS 20-50	0.46	0.00	0.01	0.05	0.02	0.03	0.04	0.12
9 J AWS 50-80	0.49	0.00	0.01	0.04	n.a.	0.00	0.03	0.09
9 J AWS Sup ice	0.46	0.03	0.03	0.15	0.02	0.00	0.03	0.19
9 J AWS Gl ice	1.26	0.00	0.01	0.27	0.03	0.34	0.03	0.58
9 J N Top 20	0.34	0.11	0.03	0.13	n.a.	0.00	0.03	0.22
9 J N 20-50	0.12	0.03	0.01	0.09	0.02	0.00	0.03	0.18
9 J N 50-80	0.50	0.02	0.01	0.03	n.a.	0.00	0.03	0.12
9 J N 80-120	0.45	0.02	0.03	0.13	n.a.	0.00	0.03	0.19
9 J N 120-137	0.26	0.02	0.04	0.15	0.02	0.00	0.03	0.16
9 J N Sup ice	0.71	0.04	0.02	0.49	n.a.	1.82	0.00	0.39

Table S4. Concentrations of cations Na^+, K^+, Mg^{2+}, Ca^{2+}, anions F^-, SO_4^{2-}, Si and DOC in ppm for each sample in late July.

Sample	Na^+	K^+	Mg^{2+}	Ca^{2+}	F^-	SO_4^{2-}	Si	DOC
30 J NW Top 20	0.56	0.02	0.02	0.20	0.04	0.00	0.00	0.14
30 J NW Gl ice	0.61	0.08	0.07	0.18	0.09	0.19	0.01	0.24
30 J SW Top 20	0.30	0.06	0.03	0.13	0.04	0.00	0.00	0.26
30 J SW Gl ice	0.62	0.03	0.11	0.36	0.04	0.17	0.00	0.14
30 J S1 Gl ice	0.99	0.12	0.36	0.85	0.04	0.25	0.00	1.81
30 J SE Gl ice	0.81	0.03	0.19	0.50	0.06	0.11	0.00	0.63
30 J NE Top	0.67	0.03	0.08	0.31	0.04	0.00	0.00	0.50
30 J NE Gl ice	0.75	0.03	0.11	0.36	0.05	0.30	0.00	0.18
30 J AWS Top	0.44	0.02	0.06	0.36	0.07	0.19	0.01	0.60
30 J AWS Sup ice	0.37	0.03	0.06	0.30	0.03	0.13	0.00	0.20
30 J AWS Gl ice	1.69	0.07	0.25	1.21	0.04	0.58	0.00	0.27
30 J N Top 20	1.39	0.04	0.05	0.35	0.08	0.00	0.00	0.32
30 J N 20-35	0.82	0.04	0.03	0.22	0.04	0.00	0.00	0.14
30 J N Gl ice	0.61	0.03	0.08	0.23	0.06	0.33	0.00	0.27

References From The Supporting Information

Felip, M. *et al.* (2007) 'Suitability of flow cytometry for estimating bacterial biovolume in natural plankton samples: Comparison with microscopy data', *Applied and Environmental Microbiology*, 73(14), pp. 4508–4514. doi: 10.1128/AEM.00733-07.

Posch, T. *et al.* (2001) 'Precision of bacterioplankton biomass determination: A comparison of two fluorescent dyes, and of allometric and linear volume-to-carbon conversion factors', *Aquatic Microbial Ecology*, 25(1), pp. 55–63. doi: 10.3354/ame025055.